PHYSICAL REVIEW B **78**, 161403(R) (2008)

Adsorption of linear chain molecules on carbon nanotubes

E. S. Alldredge, Ş. C. Bădescu,* N. Bajwa, F. K. Perkins, E. S. Snow, and T. L. Reinecke
Naval Research Laboratory, Washington, DC 20375, USA

J. L. Passmore and Y. L. Chang
Nanomix, Incorporated, Emeryville, California 94608, USA

(Received 3 July 2008; revised manuscript received 29 August 2008; published 13 October 2008)

We investigate molecular adsorption on single-walled carbon nanotubes (NTs) by *ab initio* calculations and by measurements of the conductivity response of NT arrays to trace vapors for a range of linear chain molecules. Experiment and calculations show that the short-time responses give adsorption energies that increase linearly with the molecular length. This systematic dependence indicates that the initial adsorption occurs on the defect-free regions of NTs and that these regions can play an important role in the adsorption process on NTs.

DOI: 10.1103/PhysRevB.78.161403 PACS number(s): 73.22.−f, 68.43.−h, 81.07.De, 85.35.Kt

Single-walled carbon nanotubes (NTs) have been of great interest for their novel physical properties, including high conductivity and strength,[1] as well as for a range of potential technologies based on them.[2,3] For most applications, such as electronics and sensing, however, the properties of NTs need to be modified, and their large surface-to-volume ratios mean that functionalization by surface adsorption is a powerful tool for doing so. In addition, molecular adsorption lies at the heart of sensing with NTs. To date, however, adsorption on NT systems is only beginning to be understood.

The surfaces of NTs contain covalent sp^2-like bonding between carbon atoms in a rigid structure that is almost chemically inert. As a result, adsorption on pristine NTs should be expected to be weak. Nevertheless, large adsorption energies were found in some experiments, and sensors were made from NT systems.[2–5] Early calculations for molecular adsorption on perfect NTs gave a wide range of adsorption energies.[6–11] Recent calculations have found weak binding on defect-free NTs, particularly for physisorption,[5,12,13] while recent experimental work indicates that defects on the NTs may play a role in giving strong adsorption sites on NTs.[5] The relative roles of pristine regions on NTs and of defects as adsorption sites in a full picture of molecular adsorption on NTs are not yet understood.

In this Rapid Communication, we address molecular adsorption on NT systems, particularly the role of defect-free regions in initial adsorption processes. We systematically study varying sets of linear molecules on NT arrays. These molecules include the *n*-alkanes $H(CH_2)_mH$, 1-alcohols $H(CH_2)_mOH$, and 2-ketones $H(CH_2)_{m-2}(CO)(CH_2)H$. These are linear chains of alkyls (CH_2) and differ by the addition of a hydroxyl (OH) or carbonyl (CO) group. As long closed-shell molecules with large contact areas on NTs, they provide a way to understand the role of adsorption on the extended defect-free regions in NT systems. We use calculations for molecular adsorption on NTs and measured conductance responses of NT arrays exposed to small fluxes of molecules to study adsorption for a range of molecular lengths ($m=1,9$). *Ab initio* calculations performed with density-functional theory methods on single NTs show that these molecules lie flat on the NT surface and that the adsorption energy E_{ads} depends linearly on molecular length. Measured initial responses for NT arrays are interpreted with a simple kinetic model and indicate that adsorption energies are linearly dependent on molecule length. Experiment and calculation are in good accord for the incremental adsorption energy for each alkyl group added to the molecular chain. These results indicate that the initial adsorption occurs predominantly on the defect-free NT sidewalls.

For our calculations we used the NWCHEM code.[14] This is based on localized basis sets of electronic functions and incorporates a recent density functional appropriate for noncovalent bonds. We choose two representative NTs with different chiralities and different average diameters [NT(5,5) and NT(8,0)] for the calculations. Optimized geometries of ideal NTs are obtained using periodic boundary calculations. These results are then cut to finite-length clusters, which are terminated with hydrogen atoms and are used to treat the adsorption. For each molecule the adsorption energy is determined by $E_{ads}=E_{NT+mol}-(E_{NT}+E_{mol})$, where E_{NT} is the energy of the frozen NT, E_{mol} is the energy of the free relaxed molecule, and E_{NT+mol} is the energy of the molecule relaxed upon the frozen nanotube. We use the ONIOM technique[15] to split the system into two regions, treated self-consistently with different chemical accuracies. The chemically relevant region in the center (insets of Figs. 1 and 2) contains the adsorbed molecule and a large region with 14 carbon rings underneath it and is described using hybrid density-functional M05-2X (Ref. 16) and the 6-31G(d,p) basis. This functional has been designed for treating weak noncovalent interactions between molecules.[17] The remote environment is used to obtain accurate electronic boundary conditions on the cluster and is described at the Hartree-Fock level with the STO-2G basis.

Calculated adsorption energies as functions of molecule length *m* on the pristine sidewalls of NT(5,5) and NT(8,0) are shown in Figs. 1 and 2. We find that these linear molecules have adsorption energies ranging from below 100 to above 400 meV (characteristic of noncovalent bonds). Also, we find a small charge redistribution between the molecules and NT, which is characteristic of physisorption. For the systems considered here, the Mulliken charge on the adsorbate molecules is approximately $0.1e$. The adsorption proceeds

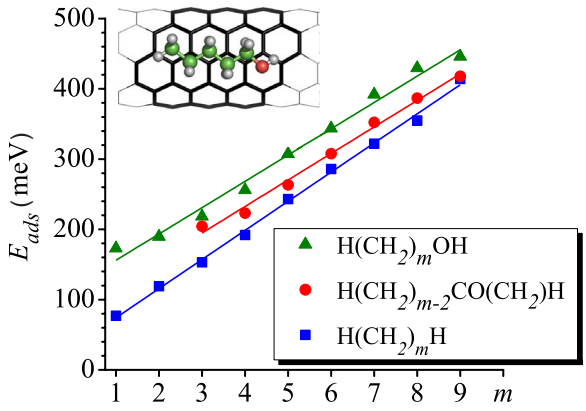

FIG. 1. (Color online) Calculated adsorption energies E_{ads} on NT(5,5) for *n*-alkanes, 1-alcohol, and 2-ketone derivatives vs the number m of C atoms in the molecule.

primarily via van der Waals forces and by forces induced by the dipole moment of the functional group (OH or CO). There is no π-π stacking, and also hydrogen bonding is not involved because the NT sidewall is not electronegative. The alcohols have the largest adsorption energies followed by ketones and then alkanes. This is due to forces induced by the permanent dipoles of alcohols and ketones. For alkanes, the attractive forces arise from electronic density fluctuations that are represented in the kinetic part of the M05-2X functional.[16] The calculated incremental adsorption energy per alkyl group E_{CH_2} is shown in Table I for the three groups (homologous series).[18]

The optimal adsorption configurations on pristine sidewalls have the carbon chains lying flat above the NT and staggered relative to the C-C bonds below them (inset of Fig. 1). This configuration can be obtained on armchair NTs such as the NT(5,5) with the linear molecule running along the length of the NT, while it can be realized on zigzag NTs such as the NT(8,0) only by small molecules ($m \leq 3$). For larger molecules, the staggered orientation on NT(8,0) is energetically unfavorable—the preferred orientation being aligned along the NT axis as shown in the inset of Fig. 2. This orientation involves a mismatch between the molecular chain

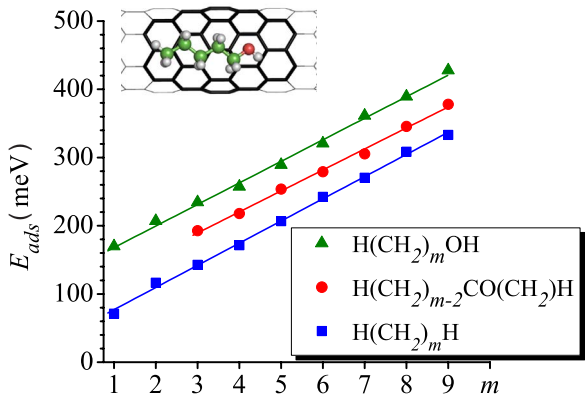

FIG. 2. (Color online) Calculated adsorption energies E_{ads} on NT(8,0) for *n*-alkanes, 1-alcohol, and 2-ketone derivatives vs the number m of C atoms in the molecule.

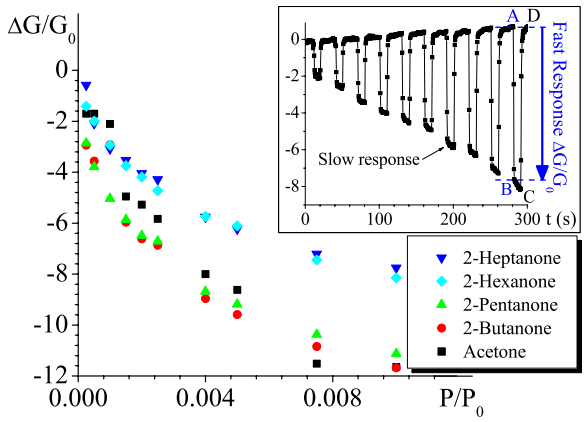

FIG. 3. (Color online) Values of the fast responses $\Delta G/G_0$ at room temperature as functions of normalized pressure P/P_0 for sequential doses from 1×10^{-4} to 0.5 and for a series of 2-ketones $[\text{H(CH}_2)_{m-2}\text{CO(CH}_2)\text{H}]$ from $m=3$ (acetone) to 7 (heptanone). P_0 is the equilibrium vapor pressure of each ketone. The inset is normalized response for 2-hexanone vs concentration including the slow response.

and the topology of the underlying NT which results in adsorption energies being slightly smaller on the NT(8,0) than on the NT(5,5), with the difference more evident for longer molecules. This is reflected in the larger values for E_{CH_2} for NT(5,5) in Table I. As a limiting case of NT size, we have calculated adsorption energies on a NT of infinite radius, i.e., a graphene sheet. In the case of alcohols in the optimal staggered orientation, the adsorption energy per additional alkyl group is $\approx$50 meV, compared to the 38 meV found on NT(5,5), giving only a modest effect from nanotube curvature.

Measurements of the conductance response of NT-network sensors to the adsorption of alkanes or alkane derivative gases have been made. We use NTs from two sources. The first set of samples has random NT networks fabricated at Naval Research Laboratory (NRL) via chemical vapor deposition (CVD) on a 30-nm-thick thermal oxide layer on a 0.001 Ω cm silicon substrate. The second set of samples were grown by CVD at Nanomix. Using standard photolithography lift-off and etching techniques, an interdigitated array of Ti/Au electrodes is deposited on top of each NT network. These procedures have been described in detail earlier.[3,19] The conductance G of the NT network is measured with a lock-in amplifier tuning the ac bias voltage at 700 Hz to maintain a current of 5 μA across the sensor. Dilute vapors are delivered to the sensors by bubbling a low

TABLE I. Theoretical values of adsorption energy per alkyl group $E_{\text{ads}}^{\text{CH}_2}$ in meV and experimental value $E_{\text{exp}}^{\text{CH}_2}$ from the average of measurements on Nanomix and NRL-NT networks.

	Alkanes		Ketones		Alcohols	
	NT(8,0)	NT(5,5)	NT(8,0)	NT(5,5)	NT(8,0)	NT(5,5)
$E_{\text{ads}}^{\text{CH}_2}$	32	41	32	38	31	38
$E_{\text{exp}}^{\text{CH}_2}$	37		24		30	

flow of dry air through liquid alkane, alcohol, or ketone and mixing this saturated vapor with a high flow of dry air.

The relative conductance change $\Delta G/G_0$ for a NT array at room temperature in response to increasing concentrations of ketones is shown in Fig. 3. The time dependence of the conductance response to increasing concentrations of hexanone is shown as an inset. The response has two stages. First, there is a discrete fast response, which occurs within the first second after the analyte vapor stream is mixed into the clean dry air on the SWNT sensor. This portion is quickly recoverable upon removal of the stream. Second, there is a portion of the conductance response that increases slowly for several seconds after the analyte vapor is added and then also slowly recovers upon removal. Based on a previous work,[5] we attribute this slow response to clustering of adsorbates at defect sites. We also find that the fast response from the polar adsorbates (alcohols and ketones) is several times larger than that from the alkanes with conductivity decreasing in the former case and slightly increasing in the latter.

We suggest that the fast recoverable response can result from adsorption and desorption on the defect-free regions of the nanotubes. To interpret the fast response data, we use a simple kinetic model in which we take the NT conductance change to be proportional to the adsorbate population on the NT surface and to the perturbation g induced by a single molecule,

$$\Delta G/G_0 \propto \Phi \cdot \tau \cdot g(\Delta\mu, \Delta Q). \tag{1}$$

Here, Φ is the molecular flux and τ is the average residence time of the adsorbate. g includes the effects of scattering on the mobility μ and of charge transfer ΔQ on the carrier density. The residence time is taken to have the form of a Boltzmann factor $\tau \propto e^{E_{\exp}/k_B T}$, where $E_{\exp}$ represents the adsorption energy per molecule and T is the room temperature. To determine the dependence of $E_{\exp}$ on m within a given homologous series, we fix a value of the response $\Delta G/G_0$ and determine the molecular flux Φ for that response as a function of m. From $\Phi|_{\Delta G/G_0} \propto 1/\tau g$ we obtain

$$\ln(\Phi)|_{\Delta G/G_0} = \text{constant} - \frac{E_{\exp}}{k_B T} - \ln g. \tag{2}$$

Values of $\ln(\Phi)|_{\Delta G/G_0}$ determined in this way are shown as a function of m in Fig. 4.

We see in Fig. 4 that the dependence on molecule length m of $\ln(\Phi)$ is nearly linear. This can be understood if the main dependence on m in Eq. (2) is from the adsorption energy such that $E_{\exp} \approx E_0 + mE_{\exp}^{CH_2}$ with only weak dependence on m from $\ln g$. This is consistent with the dependence on m found in the calculations. We obtain experimental values of the adsorption energy per added alkyl E_{CH_2} for each group of adsorbates from the slopes of linear fits to the data in Fig. 4. The averages over the two sample sets are shown with the results from the calculations in Table I. They are generally in good accord. The differences between them arise from the experiments having been done on NT arrays containing a variety of sizes and chiralities.

Thus both experiment and calculations give a linear dependence of the molecular binding energy on the number of

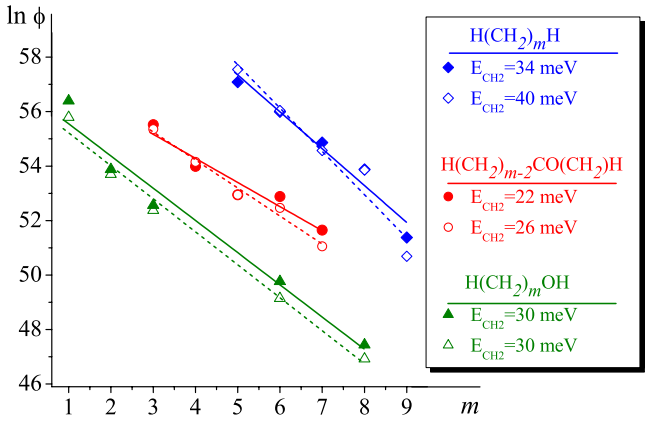

FIG. 4. (Color online) Logarithm of the molecular flux (Φ) for a fixed value of the response $\Delta G/G_0$ vs the number m of C atoms in the molecule. For alcohols and ketones we chose $\Delta G/G_0 = -3 \times 10^{-4}$. Filled or empty symbols correspond to NRL or Nanomix NTs. The fits provide the dependence of the binding energy $E_{\exp}^{CH_2}$ linear with m.

CH_2 groups in these molecules. In contrast, our calculations show that the energies of adsorption at typical oxygenation and intrinsic defects such as the carboxylic defect are larger (1 eV or more) and are independent of molecular length. This lack of length dependence is due to the large distance of these defects from the surface and to the directional bonding, which do not allow the molecule to align with the NT surface. Thus our results suggest a physical picture in which these linear molecules predominantly lie flat on the defect-free regions of the NTs with the binding energy controlled by the CH_2 groups. This shows that the defect-free regions of the NTs can play an important role in the initial adsorption of closed-shell adsorbates on NTs.

Finally, we note that the experiments also indicate that polar adsorbates give a larger effect on conductivity as shown by the smaller flux needed in Fig. 4 to reach the same change in conductance. From this we observe that changes in conductivity are given mainly by the functional groups of the polar adsorbates. The magnitude of the fast response for the polar molecules (alcohols and ketones) is larger than that of the nonpolar alkanes and the sign of the response is opposite in the two cases, with conductance for the polar molecules decreasing and that of the nonpolar molecules increasing with adsorbate concentration. These differences cannot be explained by differences in the adsorption energies. Also, our calculations do not give large differences in the charge transfer in the cases of polar and nonpolar adsorbates. These results indicate that changes in the scattering mechanisms occur upon adsorption particularly for the polar molecules. We suggest that this could be from additional scattering from the polar adsorbates. To illustrate this, we employ a simple tight-binding description of the scattering.

We use our *ab initio* calculations for the charge transfers and for the dipole scattering matrix elements in the Boltzmann equation in a simple tight-binding model. Adding a small concentration of adsorbed molecules gives a change in carrier concentration $\delta\Lambda$ and a change in carrier mobility $\delta\mu$. These determine a change in conductance of $\sigma \approx \sigma_0 + \delta\sigma^{(\mu)}$

$+\delta\sigma^{(\Lambda)}$ with $\sigma_0=\mu_0\Lambda_0$, $\delta\sigma^{(\mu)}=\delta\mu\Lambda_0$, and $\delta\sigma^{(\Lambda)}=\mu_0\delta\Lambda=\sigma_0\delta\Lambda/\Lambda_0$. Here μ_0 and Λ_0 denote the intrinsic mobility and carrier density of an assumed *p*-doped NT. We find that the ratio of the change in the scattering to the change in the concentration is

$$\frac{\delta\sigma^{(\mu)}}{\delta\sigma^{(\Lambda)}}=-\frac{\mu_0 a^2\hbar}{\tilde{A}^2\pi}\frac{\langle|\widetilde{H_{kk'}}|^2\rangle}{\delta q}, \tag{3}$$

where $\langle|\widetilde{H_{kk'}}|^2\rangle$ is the average scattering amplitude at the Fermi surface, $\tilde{A}$ is a parameter obtained by averaging over NTs of different sizes, and a is the ideal lattice constant of graphene. (δq is the charge transfer per molecule to the carrier density of the NT and is obtained from the change in the Mulliken charge on the adsorbate in our electronic calculations.) This establishes a limiting case where all charges transfer is into the carrier density of the NT in order to estimate the maximum possible effect on conduction from charge transfer. The mobility μ_0 for a typical single ideal NT can be as large as $\mu_0\sim 1\times 10^4$ cm^2/Vs.[1] In this case the ratio in Eq. (3) is $\sim -1\times 10^4$, which indicates that the induced dipole scattering can have a large effect in this case. For the present samples of NT arrays, the measured mobility is smaller, $\mu_0\approx 30$ cm^2/Vs, due to scattering at junctions, etc. Using this value as an average for a NT and considering, for example, a distribution of zigzag NT(n,0) and metallic NT(n,n) with n from 5 to 15 in Eq. (3), we obtain $\delta\sigma^{(\mu)}/\delta\sigma^{(\Lambda)}\sim -3.2$. This ratio is larger if the average is taken over smaller NTs. Thus we see in this model that the dipole scattering gives a change in conductivity that is opposite in sign from that of the charge transfer.[20] This is consistent with the negative sign seen for the ratio of the conductivity response in the experiments here for the nonpolar molecules to that for the polar adsorbates.

We have shown through *ab initio* calculations and conductance measurements that the adsorption energies of linear alkane, alcohol, and ketone molecules increase linearly with the length of the molecule. These results suggest that initial adsorption occurs with molecules predominantly lying flat on defect-free regions of the nanotubes. Differences in conductivity responses for polar and nonpolar adsorbates were traced to changes in scattering due to adsorbates.

This work was supported in part by ONR and DTRA. E. S. Alldredge is supported by NRC/NRL, and N. Bajwa is supported by ASEE/NRL. We acknowledge the support of the DoD High Performance Computing system for the calculations and also useful discussions with Victor Bermudez.

*Corresponding author; stefan.badescu@nrl.navy.mil

[1] J. Charlier, X. Blase, and S. Roche, Rev. Mod. Phys. **79**, 677 (2007).

[2] J. Kong, N. Franklin, C. Zhou, M. Chaline, S. Peng, K. Cho, and H. Dai, Science **287**, 622 (2000).

[3] E. Snow, F. Perkins, E. Houser, Ş. C. Bădescu, and T. Reinecke, Science **307**, 1942 (2005).

[4] E. Snow and F. Perkins, Nano Lett. **5**, 2414 (2005).

[5] J. Robinson, E. Snow, Ş. C. Bădescu, T. Reinecke, and F. Perkins, Nano Lett. **6**, 1747 (2006).

[6] J. Zhao, A. Buldum, J. Han, and J. Lu, Nanotechnology **13**, 195 (2002).

[7] J. Zhao, J. Lu, J. Han, and C. Yang, Appl. Phys. Lett. **82**, 3746 (2003).

[8] P. Giannozzi, Appl. Phys. Lett. **84**, 3936 (2004).

[9] S. H. Jhi, S. G. Louie, and M. L. Cohen, Phys. Rev. Lett. **85**, 1710 (2000).

[10] M. Grujicic, G. Cao, and R. Singh, Appl. Surf. Sci. **211**, 166 (2003).

[11] N. Chakrapani, Y. Zhang, S. Nayak, J. Moore, D. Carrol, Y. Choi, and P. Ajayan, J. Phys. Chem. B **107**, 9308 (2003).

[12] F. Tournus and J. C. Charlier, Phys. Rev. B **71**, 165421 (2005).

[13] L. M. Woods, Ş. C. Bădescu, and T. L. Reinecke, Phys. Rev. B **75**, 155415 (2007).

[14] E. J. Bylaska *et al.*, NWChem, *A Computational Chemistry Package for Parallel Computers, Version 5.1* (Pacific Northwest National Laboratory, Richland, WA, USA, 2007). http://www.emsl.pnl.gov/docs/nwchem/nwchem.html

[15] We use the ONIOM (Our Own *n*-layered Integrated Molecular Orbital and Molecular Mechanics) method as implemented in M. Svensson, S. Humbel, R. D. J. Froese, T. Matsubara, S. Sieber, and K. Morokuma, J. Phys. Chem. **100**, 19357 (1996).

[16] Y. Zhao, N. E. Schultz, and D. G. Truhlar, J. Chem. Theory Comput. **2**, 364 (2006).

[17] Y. Zhao and D. G. Truhlar, J. Chem. Theory Comput. **3**, 289 (2007).

[18] We have tested two possible corrections to our calculations, the use of the larger 6-31++G(d,p) basis and a correction for the basis set superposition error (BSSE). Using these, we find that adsorption energies can decrease up to 25%, while the dependence of the adsorption energy on length typically changes by only a few meV. For example, for the alcohols, we find roughly a 50 meV decrease in absolute adsorption energies, while the value $E_{\mathrm{exp}}^{\mathrm{CH_2}}$ in Table I decreases from 38 meV to 35 meV per CH_2. These modifications do not change the physical picture of weak physisorption with linear changes in the adsorption energies.

[19] J. Robinson, E. Snow, and F. Perkins, Sens. Actuators, A **135**, 309 (2007).

[20] We also considered symmetric molecules with a CO group at each end that give a zero net molecular dipole: 2,5-hexanedione $CH_3(CO)(CH_2)_2(CO)CH_3$ and 2,3-butanedione $CH_3(CO)_2CH_3$. Our calculated adsorption energies are only slightly larger than those calculated for the asymmetric 2-hexanone and 2-butanone. The calculated charge transfers to NTs are larger than those from the 2-ketones considered above. Nevertheless, the measured fast responses are much smaller than those of the ketones. This supports the picture in which the dipole scattering contributes significantly to the conductance response.